



Research Papers

Analysis of natural convection and the generation of entropy within an enclosure filled with nanofluid-packed structured pebble beds subjected to an external magnetic field and thermal radiation

Mehdi Hashemi-Tilehnoee^{a,*}, Seyyed Masoud Seyyedi^{b,c}, Elena Palomo del Barrio^{a,d},
Mohsen Sharifpur^{e,f,**}

^a Centre for Cooperative Research on Alternative Energies (CIC energiGUNE), Basque Research and Technology Alliance (BRTA), Alava Technology Park, Albert Einstein 48, 01510 Vitoria-Gasteiz, Spain

^b Department of Mechanical Engineering, Aliabad Katoul Branch, Islamic Azad University, Aliabad Katoul, Iran

^c Energy Research Center, Aliabad Katoul Branch, Islamic Azad University, Aliabad Katoul, Iran

^d IKERBASQUE Basque Foundation for Science, Plaza Euskadi 5, 48009 Bilbao, Spain

^e Department of Mechanical and Aeronautical Engineering, University of Pretoria, Pretoria 0002, South Africa

^f Department of Medical Research, China Medical University Hospital, China Medical University, Taichung, Taiwan



ARTICLE INFO

Keywords:

Natural convection
Entropy generation
Pebble
Magnetic field
Thermal radiation
Packed bed

ABSTRACT

The efficient heat transfer and energy storage during periods of excess energy production, like peak solar or wind power generation, is facilitated by the compact design and closely packed pebble bed thermal energy storage system. This study focuses on analyzing natural convection and entropy generation in a closed chamber filled with water/Al₂O₃-water nanofluid containing eight spherical pebbles arranged in a structured manner, referred to as packed beds while considering the presence of an external magnetic field and surface thermal radiation. The single-phase and two-phase models for nanofluid equations are solved using Ansys Fluent, employing a non-dimensional approach for the calculations and presenting the results. Two cases with two-dimensional cavities in the presence of a magnetic field and conductive solid blocks are considered for validating the numerical method. Besides two-dimensional cases, another three-dimensional case is considered to evaluate heat transfer for the air-filled cubic cavity. The active parameters are the Hartmann number, Rayleigh number, and solid-to-liquid thermal conductivity ratio. The findings are displayed for different parameters, encompassing the mean Nusselt number, generation of entropy, mean Bejan number, patterns of isotherms, velocity distribution, and localized entropy generation. The averaged Nusselt number decreases by approximately 2 % when applying a magnetic field. However, thermal radiation partially compensates for the negative effect of the strong magnetic field. At a Rayleigh number (Ra) of 10⁶, entropy generation increases by 18 % due to radiation and by 78 % because of the magnetic field. The average Bejan number increases from approximately 0.02 to 0.36 while the Hartmann number increases from 0 to 100 for a single-phase nanofluid without radiation effect.

1. Introduction

As our world grows towards renewable energy sources, the demand for effective energy storage technologies rises. Energy storage systems are crucial in connecting the gap between energy generation and utilization, facilitating the assimilation of intermittent renewable sources, and ensuring a dependable and steady power supply. When it comes to storing energy, using packed pebble bed technology seems like a great

option. This method has many benefits, including high thermal efficiency, quick response times, affordability, and the ability to scale up easily [1]. Packed beds find extensive application across various industries, including chemical reactors, distillation processes, waste heat recovery, hydrogen production, and dust removal devices [2–4]. Random packed beds are often favored for their ease of construction and operation, but there has been growing interest in structured packed beds due to their unique abilities and potential uses in recent years. There

* Corresponding author.

** Correspondence to: M. Sharifpur, Department of Mechanical and Aeronautical Engineering, University of Pretoria, Pretoria 0002, South Africa.

E-mail addresses: mhashemi@cicenergigune.com (M. Hashemi-Tilehnoee), mohsen.sharifpur@up.ac.za (M. Sharifpur).

<https://doi.org/10.1016/j.est.2023.109223>

Received 24 August 2023; Received in revised form 2 October 2023; Accepted 5 October 2023

Available online 11 October 2023

2352-152X/© 2024 CIC ENERGIGUNE. Published by Elsevier Ltd.

(<http://creativecommons.org/licenses/by-nc-nd/4.0/>).

This is an open access article under the CC BY-NC-ND license

have been numerous investigations conducted on the flow, heat, and mass transfer in both random and structured packed beds. These studies have shown that the hydrodynamic and heat transfer performances in these two types of beds are quite distinct. Specifically, the research indicates that the pressure drop in structured packed beds is typically much lower, resulting in better overall heat transfer performance [5] [6]. When it comes to energy storage, pebbles made of materials with high heat storage capabilities, such as high-density ceramics or advanced phase change materials, are used. Understanding the flow behavior in a packed bed is crucial. In certain instances, the passive heat transfer mechanism within a packed pebble bed can be very intricate, involving heat conduction, radiation, and natural convection at the pore level. Despite its complexity, this is a fascinating subject [7]. Several studies have examined the effects of natural convection on the structured packed pebble bed and its impact on individual pebbles. Laguerre et al. [8] examined transient heat transfer in a packed bed of spheres through free convection using two numerical methods. The first method involved using Ansys Fluent software and the second method, developed by the authors, employed techniques designed for porous media and packed beds. Both approaches yielded numerical results that aligned well with experimental measurements. A study conducted by Bu et al. [7] in 2020 examined the effective thermal conductivity (ETCs) of high-temperature pebble-bed reactors in the passive heat transfer mode of cooling. The research revealed that natural convection has a positive impact on ETCs in the bulk region, but a negative impact in the near-wall region. Qu et al. [1] examined the mixed convective heat transfer occurring in a structured packed bed of aluminum spheres under unsteady conditions. According to their research, natural convection has a significant impact on mixed convective heat transfer. In 2023, a study by Qu et al. [9] examined the behavior of velocity and density fields in a packed bed with varying pebble sphere diameters. By analyzing how physical parameters affect mixed convective heat transfer, the research found that natural convection has a greater impact on heat transfer when there is a higher temperature difference between the fluid and solid, larger particle diameters, or decreased fluid temperature. One of the important mechanisms which should be carefully applied to the packed bed natural convection analysis is radiation between solid surfaces. There are many papers in that researchers studied the effect of radiative heat transfer on two or three-dimensional double-diffusive convection [10–17]. Besides considering thermal radiation, some researchers used the negative impact of the magnetic field on three-dimensional fluid flow to suppress the convective flow and the heat transfer rate [18]. The magnetic field or the Hartmann number can be applied to the geometries as an external source or as a vector to a specified direction [19–28]. This study focuses on analyzing natural convection and entropy generation in a cavity filled with Al_2O_3 -water nanofluid and containing structured pebbles as a packed bed. The presence of surface thermal radiation and a magnetic field is considered in the analysis. The heat transfer occurs between two hot and cold walls of the enclosure. The equations of fluid and energy are solved for single-phase and two-phase nanofluid, taking into account the impacts of radiation and magnetic field as source terms. This is accomplished using Ansys Fluent CFD software and a non-dimensional approach. The geometry mesh is validated against previous works in the literature. The study will present results in the form of Nusselt number, isotherms, velocity, entropy generation, and Bejan number. The impact of solid-to-fluid thermal conductivity will also be discussed in the results. The advantages of the present study with respect to many previous works can be summarized as follows:

- A 3D industrial complex geometry of a packed pebble bed, where the pebbles serve as conducting media, is chosen for modeling.
- Entropy generation analysis is conducted using the non-dimensional approach with Ansys Fluent.
- Both single-phase and two-phase approaches for nanofluid modeling are taken into consideration.

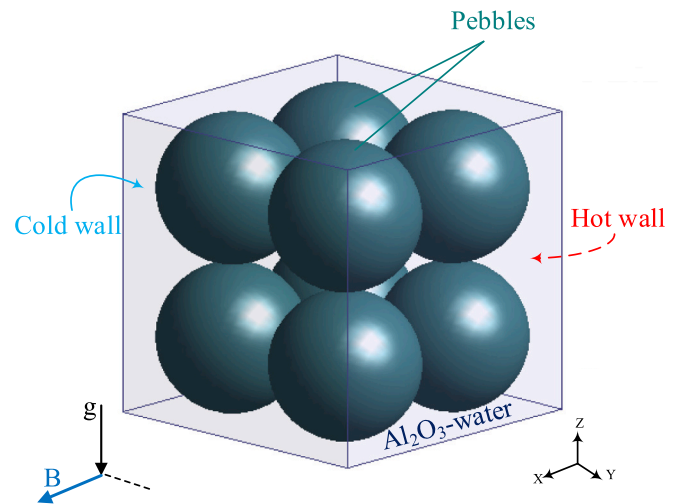


Fig. 1. The problem setup, featuring eight pebbles and the direction of the applied magnetic field.

- The study focuses on investigating the effects of the magnetic field and surface thermal radiation.

2. Definition of the geometric configuration

The schematic of the cubic enclosure filled with Al_2O_3 -water is illustrated in Fig. 1. In the figure, two vertical walls, indicated as hot and cold walls (T_h and T_c) have fixed temperatures. The remaining walls of the enclosure are thermally isolated. Within the enclosure, there is a typical configuration of eight conductive spherical blocks, forming a structured packed bed medium. Additionally, a uniform magnetic field is applied to the cavity in parallel to the OX direction. The modeling of heat transfer involves considering three types of mechanisms: solid/fluid conduction, radiation between solid surfaces, and natural convection.

3. Mathematical formulation

In this study, the fluid flow is characterized as three-dimensional, laminar, Newtonian, steady, and incompressible. For the sake of simplicity, certain factors like viscous dissipation, Joule heating, and induced electric current are omitted. The governing equations are obtained by using the Boussinesq approximation and integrating a uniform magnetic field and thermal radiation for the gray and diffuse surfaces. The overarching formulations of these governing equations are employed for both single-phase and two-phase mixture models, which are employed to represent the nanofluids.

3.1. Single-phase approach

In the single-phase approach, the nanofluid is treated as a homogeneous fluid. The conservation equations for mass, momentum, and energy are expressed as Eqs. (1)–(4) [29,30]:

$$\nabla \cdot \vec{V} = 0 \tag{1}$$

$$\rho_{nf} \nabla \cdot (\vec{V} \vec{V}) = -\nabla p + \nabla \cdot (\mu_{nf} \nabla \vec{V}) - (\rho\beta)_{nf} \vec{g} (T - T_0) + \vec{F}_{MF} \tag{2}$$

$$(\rho C_p)_{nf} (\vec{V} \nabla T) = \nabla \cdot (k_{nf} \nabla T) + S_r \tag{3}$$

$$\nabla \cdot (k_s \nabla T) + S_r = 0 \tag{4}$$

where $\vec{F}_{MF} = \vec{J} \times \vec{B} = \sigma_{nf} (\vec{V} \times \vec{B}) \times \vec{B}$ [31] and $S_r = -\nabla \cdot q_r$. The

surface-to-surface (S2S) radiation model is adopted to calculate the radiation heat transfer, as described in references [4,30]. In this model, the energy exchange between two surfaces depends on their size, separation distance, and orientation, which is accounted for by a geometric function known as the “view factor.” The primary assumption of the S2S model is that any absorption, emission, or scattering of radiation can be neglected. Therefore, the analysis only considers surface-to-surface radiation. The surface emissivity (ϵ) of the graphite pebble surfaces and all walls is set to 0.8. In this model, the energy flux leaving a given surface comprises directly emitted energy and reflected energy. The reflected energy flux depends on the incident energy flux from the surroundings, which can be expressed in terms of the energy flux leaving all other surfaces. Mathematically, the energy leaving from surface “k” can be expressed as:

$$J_k = E_k + \rho_k \sum_{j=1}^N F_{kj} J_j \quad (5)$$

where J_k represents the energy that is given off (or radiosity) of surface k , and E_k represents the emissive power of surface k and view factor F_{kj} is the fraction of the energy leaving surface j that is incident on surface i . The view factors of all radiating surfaces are calculated based on the mesh faces in ANSYS Fluent. Also, the characteristics of homogenous single phase nanofluid can be obtained as below [32,33]:

$$\rho_{nf} = \rho_s \phi + \rho_f (1 - \phi) \quad (6)$$

$$(\rho C_p)_{nf} = (\rho C_p)_f (1 - \phi) + (\rho C_p)_s \phi \quad (7)$$

$$(\rho \beta)_{nf} = (\rho \beta)_f (1 - \phi) + (\rho \beta)_s \phi \quad (8)$$

$$\mu_{nf} = \frac{\mu_f}{(1 - \phi)^{2.5}} \quad (9)$$

$$\frac{k_{nf}}{k_f} = \frac{k_s + (m - 1)k_f - (m - 1)\phi(k_f - k_s)}{k_s + (m - 1)k_f + \phi(k_f - k_s)}, m = 3 \text{ for sphere particles} \quad (10)$$

$$\frac{\sigma_{nf}}{\sigma_f} = 1 + \frac{3\left(\frac{\sigma_s}{\sigma_f} - 1\right)\phi}{\left(\frac{\sigma_s}{\sigma_f} + 2\right) - \left(\frac{\sigma_s}{\sigma_f} - 1\right)\phi} \quad (11)$$

3.2. Two-phase approach

This model characterizes the flow through two phases: the initial phase consists of water, while the second phase is a uniform Newtonian fluid. The properties of this second phase are analogous to those of a nanoparticle suspension in water. Within this second phase, a robust interaction between the movement of nanoparticles and the fluid flow in their vicinity is presumed, resulting in the nanoparticles moving in tandem with the surrounding fluid in the second phase. So, the flow is a three-dimensional two-phase mixture in laminar, steady, and incompressible with a shared pressure. The concentration of nanoparticles in the mixture is kept low enough to disregard particle collisions and heat conduction through particle-to-particle contact. Similar to single-phase model, the magnetic field and S2S radiation model are applied to calculations. The governing equations, taking into account the assumptions mentioned above, take the following general form [30,34]:

$$\nabla \cdot (\rho_m \vec{V}_m) = 0, \vec{V}_m = \frac{\alpha_{bf} \rho_{bf} \vec{V}_{bf} + \alpha_{nf} \rho_{nf} \vec{V}_{nf}}{\rho_m}, \rho_m = \alpha_{bf} \rho_{bf} + \alpha_{nf} \rho_{nf} \quad (12)$$

$$\begin{aligned} \rho_m \nabla \cdot (\vec{V}_m \vec{V}_m) &= -\nabla p + \nabla \cdot (\mu_m \nabla \vec{V}_m) - (\rho \beta)_m \vec{g} (T - T_0) \\ &+ \nabla \cdot (\alpha_{bf} \rho_{bf} \vec{V}_{dr,bf} \vec{V}_{dr,bf} + \alpha_{nf} \rho_{nf} \vec{V}_{dr,nf} \vec{V}_{dr,nf}) \\ &+ \vec{F}_{MF}, \mu_m = \alpha_{bf} \mu_{bf} + \alpha_{nf} \mu_{nf}, \vec{V}_{dr,bf/nf} = \vec{V}_{bf/nf} - \vec{V}_m \end{aligned} \quad (13)$$

$$\begin{aligned} \nabla \cdot (\alpha_{bf} \rho_{bf} C_{p,bf} \vec{V}_{bf} + \alpha_{nf} \rho_{nf} C_{p,nf} \vec{V}_{nf}) T_m &= \nabla \cdot (k_m \nabla T_m) + S_r, k_m \\ &= \alpha_{bf} k_{bf} + \alpha_{nf} k_{nf} \end{aligned} \quad (14)$$

$$\nabla \cdot (k_s \nabla T) + S_r = 0 \quad (15)$$

The mixture model is employed in this study, which allows the model to account for phase stratification caused by gravity and phase segregation due to flow path curvature. These phenomena cannot be represented by the single-phase approach. To transform dimensional equations into non-dimensional ones, the innovation method is utilized in this study, as detailed in previous studies [35–37]. The results of isotherms, Nusselt numbers, and velocities will be presented in the results and discussion section. The non-dimensional parameters used in the calculations are presented in the following equations:

$$\begin{aligned} (X, Y, Z) &= \frac{(x, y, z)}{L}, (U, V, W) = (u, v, w) \frac{L}{\alpha_f}, Pr_f = \frac{\nu_f}{\alpha_f}, Ra_f \\ &= \frac{g \beta_f L^3 (T_h - T_c)}{\nu_f \alpha_f}, Ha_f = B_0 L \sqrt{\frac{\sigma_f}{\rho_f \nu_f}}, \theta = \frac{T - T_c}{T_h - T_c}, P = \frac{p}{\rho k \frac{\alpha}{L^2}}, R_d \\ &= \frac{4\sigma^* T_0^3}{k^* k_f} \end{aligned} \quad (16)$$

The boundary conditions by considering non-dimensional formulation take the form [38]:

$$\text{Hot wall : } U = V = W = 0, \theta = 1 \quad (17)$$

$$\text{Cold wall : } U = V = W = 0, \theta = 0$$

$$\text{Insulated walls : } U = V = W = 0, \frac{\partial \theta}{\partial Y} = 0$$

$$\text{conducting walls : } \Psi = \frac{\partial \Psi}{\partial Y} = 0, \theta = 0$$

$$\text{Solid fluid interfaces : } U = V = W = 0, \theta|_s = \theta|_f, \frac{\partial \theta}{\partial n}|_f = k_s \frac{\partial \theta}{\partial n}|_s$$

The indicators of heat transfer rate in the cavity are calculated by Nu_{ave} in the cavity and Nu_{local} (local Nusselt number) on the hot wall:

$$Nu_{local} = \frac{L q_f}{k_{nf} (T_h - T_c)}, q_f = q_c + q_r \quad (18)$$

where average Nusselt number can be calculated as below:

$$Nu_{ave} = \int_0^L \int_0^L Nu_{local}(y, z) dY dZ \quad (19)$$

3.3. Entropy generation

Entropy generation stands as the primary contributor to the inefficiency of systems. Local entropy generation can be examined using Eq. (20), and its corresponding dimensionless representation is provided by Eq. (21) [39–41]:

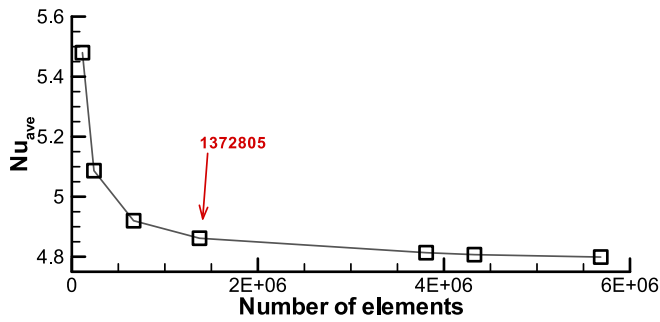


Fig. 2. Nu_{ave} versus different grid sizes.

$$\dot{S}_{gen} = \frac{k_{nf}}{T_0^2} \left[\left(\frac{\partial T}{\partial x} \right)^2 + \left(\frac{\partial T}{\partial y} \right)^2 + \left(\frac{\partial T}{\partial z} \right)^2 \right] + \frac{\mu_{nf}}{T_0} \left\{ 2 \left[\left(\frac{\partial u}{\partial x} \right)^2 + \left(\frac{\partial v}{\partial y} \right)^2 + \left(\frac{\partial w}{\partial z} \right)^2 \right] + \left(\frac{\partial u}{\partial y} + \frac{\partial v}{\partial x} \right)^2 + \left(\frac{\partial v}{\partial z} + \frac{\partial w}{\partial y} \right)^2 + \left(\frac{\partial w}{\partial x} + \frac{\partial u}{\partial z} \right)^2 \right\} + \frac{\sigma_{nf} B_0^2 (v^2 + w^2)}{T_0} \quad (20)$$

$$N_{L,gen} = \frac{\dot{S}_{gen}}{\left[\left(\frac{k_f}{T_0} \right) \left(\frac{\Delta T}{L} \right)^2 \right]} = \frac{k_{nf}}{k_f} \left[\left(\frac{\partial \theta}{\partial X} \right)^2 + \left(\frac{\partial \theta}{\partial Y} \right)^2 + \left(\frac{\partial \theta}{\partial Z} \right)^2 \right] + \frac{\mu_{nf} \Phi_f}{\mu_f} \left\{ 2 \left[\left(\frac{\partial U}{\partial X} \right)^2 + \left(\frac{\partial V}{\partial Y} \right)^2 + \left(\frac{\partial W}{\partial Z} \right)^2 \right] + \left(\frac{\partial U}{\partial Y} + \frac{\partial V}{\partial X} \right)^2 + \left(\frac{\partial V}{\partial Z} + \frac{\partial W}{\partial Y} \right)^2 + \left(\frac{\partial W}{\partial X} + \frac{\partial U}{\partial Z} \right)^2 \right\} + \frac{\sigma_{nf} Ha_f^2 \Phi_f (V^2 + W^2)}{\sigma_f} \quad (21)$$

with

$$\Phi_f = \frac{\mu_f T_0}{k_f} \left(\frac{\alpha_f}{L \Delta T} \right)^2 \quad (22)$$

As indicated in Eq. (21), local entropy generation can be broken down into three primary components linked to heat transfer ($N_{L,HT}$), fluid friction ($N_{L,FF}$) and magnetic field ($N_{L,MF}$). The local Bejan number which represents the ratio of heat transfer irreversibility to total irreversibility [40], can be expressed as follows:

$$Be_L = N_{L,HT} / N_{L,gen} \quad (23)$$

The averaged Bejan number can be computed by:

$$Be_{ave} = \frac{\int_V Be_L dV}{\int_V dV} \quad (24)$$

4. Numerical method

In Fig. 1, eight graphite pebbles with 0.5 L arranged in a $2 \times 2 \times 2$ array using the simple cubic packing rules. The purpose of the simulations is to investigate the occurrence of natural convection, radiation, and conduction in this pebble bed configuration. The natural convection phenomenon results from density variations in the Al_2O_3 -water nanofluid, which are induced by the force of gravity. The equations are solved using the ANSYS Fluent code, utilizing a pressure-based segregated finite volume method and a non-dimensional system. All the walls have a smooth surface, free of roughness. The Boussinesq approximation has been employed to approximate the buoyancy concept, while the temperature changes have been disregarded [33]. The Coupled algorithm is employed to establish a connection between the velocity and pressure fields, and the PRESTO scheme is implemented for spatial discretization of pressure [36]. In the case of viscous models, the laminar model is adopted for both single-phase and two-phase nanofluid modeling. The second-order upwind scheme was employed to incorporate the effect of convection into the coefficients within the finite-volume equations. The convergence criteria have been established at 10^{-6} . To properly model the pebbles, four typical contact point modifications are considered for investigation: gaps (particle shrinking), overlaps (particle enlarging), bridges (cylindrically bridging), and caps (sphere cap removing) treatments [42]. However, in the present study, a gaps treatment with a 0.8 % distance between particles was selected during the model building process. The purpose of this choice was to prevent the generation of low-quality meshes at the contact points between the particles. It has been found that these gaps have a minimal impact on the flow and heat transfer. According to the study conducted by Calis et al., when the gap size is 2 % of the particle size, there is a 0.5 % deviation compared to when the gap size is 1 % [5,9].

4.1. Grid check

In order to ensure a suitable mesh for the cavity, the impact of the mesh on the numerical outcomes was assessed under the conditions $Ha = 0$, $Pr = 6.2$, and $Ra = 10^6$. As depicted in Fig. 2, it was determined that a mesh comprising 1,372,805 elements or finer is essential to mitigate discretization errors in the numerical simulation, alongside double-precision approximations. Grid independence was confirmed by doubling the number of cells, resulting in an increase to 3,808,656 elements (approximately 2.7 times). Despite this increase in elements, the Nusselt number only changed by about 1 %. This indicates that the results are relatively insensitive to further mesh refinement beyond the finer mesh configuration.

Table 1 Isotherms and streamlines comparisons (*NR: non reported).

Configuration	Rayleigh number	Isotherms reported by Ref [38]	This study	Streamlines reported by Ref [38]	This study
<p>Number of Blocks = 16 Diameter to length = 0.15</p>	10 ⁶				
		$Nu_{ave} = 4.27$	$Nu_{ave} = 4.30$	NR*	$\Psi_{max} = 6.80$

Table 2
Isotherms and streamlines comparisons (*NR: non reported).

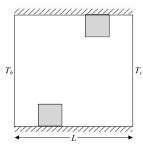
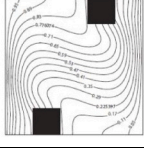
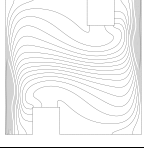
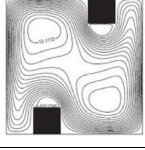

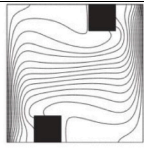
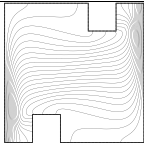
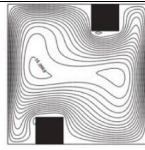
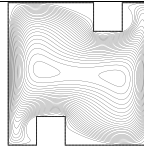
configuration	Ha	Isotherms reported by Refs [43], [44]	This study	Streamlines reported by Refs [43], [44]	This study
	0				
		Nu _{ave} = 7.30	Nu _{ave} = 7.17	NR*	Ψ _{max} = 14.35
	150				
		Nu _{ave} = 6.35	Nu _{ave} = 5.83	NR	Ψ _{max} = 9.79

Table 3
Comparison between present results and Fusegi et al. [45] for the average Nusselt number in.

	Ra=10 ³	Ra=10 ⁴	Ra=10 ⁵	Ra=10 ⁶
Reference [45]	1.085	2.100	4.361	8.770
Present study	1.071	2.061	4.374	8.862
Error (%)	-1.29	-1.85	0.29	1.04

4.2. Three tests for validation

The credibility of the suggested numerical model has been established via three distinct case studies. The primary case study revolves around a two-dimensional cavity setup, utilizing conditions that were examined by Merrikh and Lage [38]. In their investigation, Merrikh and Lage examined the phenomenon of natural convection within a square cavity that was heated on one side. This cavity is comprised of 16 solid square blocks which conduct heat, and the ratio of the thermal conductivity of these solids to that of the fluid is set to 1. The Prandtl number of the fluid is assigned as Pr = 1. The study explores Rayleigh number values of Ra=10⁶. The streamlines and isotherms, both from the previous research and calculated in the present study, are summarized in Table 1. It is noted that the streamlines, isotherms, and Nusselt number (Nu) values obtained in the current study show excellent agreement. The methodology used to evaluate the streamlines in these 2D studies is described in detail in Reference [35].

The second case entails examining the influence of a magnetic field within cavities containing 2 solid blocks. Pirmohammadi conducted studies [43,44] involving a square cavity with Pr = 0.01 and Ra = 10⁷. Although in these cases the solid blocks are adiabatic, they can still be used for the validation of the magnetic field effect. In Table 2, a comparison is provided between the streamlines and isotherms obtained by Pirmohammadi [43,44], and those computed in the current study. The presented comparison demonstrates a high degree of concurrence between the outcomes that considered the effect of the magnetic field.

In the third case, the proposed solving method is validated through

Table 4
Thermo-physical properties of Air, Water, Al₂O₃-nanoparticle [33], Al₂O₃-water nanofluid (3 %).

	ρ(kg/m ³)	k(W/mK)	σ(μS/cm)	Pr	C _p (J/kgK)	β(K ⁻¹)
Pure water	997.1	0.613	0.05	6.2	4179	2.1 × 10 ⁻⁴
Al ₂ O ₃	3970	40	1 × 10 ⁻¹⁰	-	765	0.85 × 10 ⁻⁵
Al ₂ O ₃ -water nanofluid (3 %)	1235	0.65	0.04	4.91	3355	1.6 × 10 ⁻⁴

three-dimensional natural convection analysis in a cubic air cavity, as previously studied by Fusegi et al. [45]. Table 3 presents a comparison of the overall Nusselt number on the hot wall at different Rayleigh numbers.

The comparison demonstrates good agreement between the present results and the benchmark results obtained by Fusegi et al. [45]. The maximum relative error observed is <2 %, which is considered acceptable for engineering applications. This validation process confirms the accuracy and reliability of the proposed solving method for three-dimensional natural convection analysis in cubic air cavities. Overall, the numerical model shows promising performance by producing results that closely match the reference data, and it can be confidently applied for various engineering applications involving natural convection in complex geometries.

5. Results and discussions

In the current research, the focus is on conducting simulations to study natural convection and entropy generation in a complex cubic packed pebble bed that is filled with water and other case with 3 % Al₂O₃-water nanofluid. Two different nanofluid modeling approaches are employed: single-phase flow and two-phase flow. These approaches involve solving the conservation equations using the ANSYS Fluent software with a non-dimensional scheme. The simulations also consider surface radiation effects between the walls of the pebbles. To explore the influence of a magnetic field, two different Hartmann numbers (Ha) are considered, namely Ha = 0 and Ha = 100. The magnetic field vector is oriented along the OX direction. The study investigates the behavior of the system under different Rayleigh number (Ra) conditions. The Rayleigh number values explored are Ra = 10⁴, Ra = 10⁵ and Ra = 10⁶. In addition, the thermal conductivity ratio (K) changes for K = 0.5, 1, 5, 10, 50, and 100. Furthermore, the irreversibility distribution ratio (Φ) is taken Φ = 10⁻⁴. The fluid properties of the base fluid (water) and the Al₂O₃ nanoparticles are specified in Table 4.

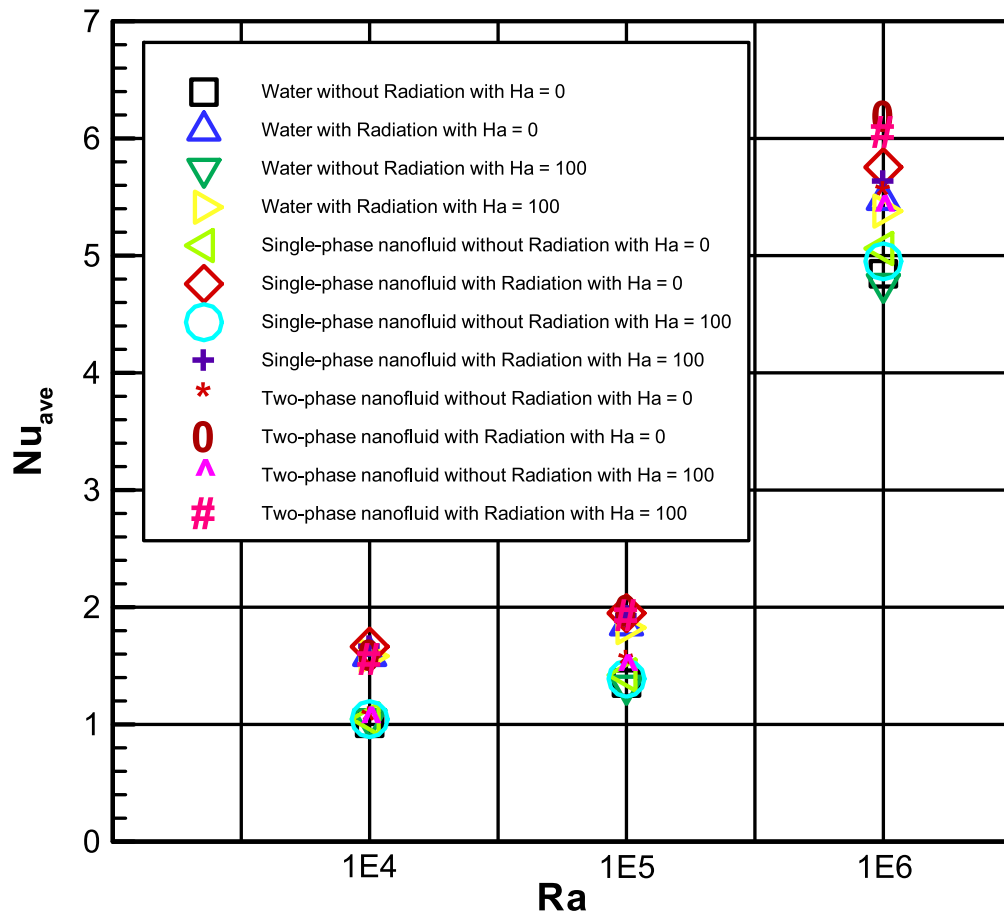


Fig. 3. Average Nusselt number with respect to Rayleigh number with/without Ha for water, single-phase and two-phase conditions.

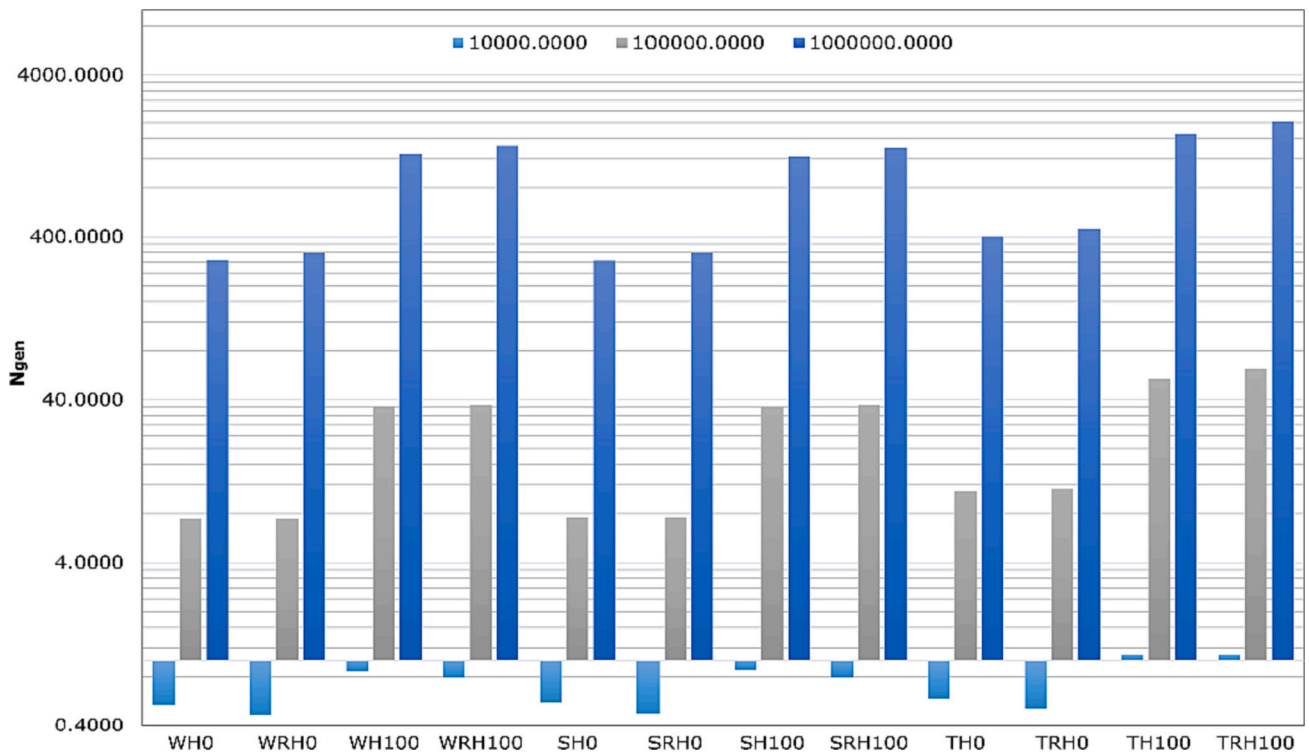


Fig. 4. The entropy generation number with respect to Rayleigh number with/without Ha for water, single-phase and two-phase conditions (W: water, H: Hartmann, S: single-phase nanofluid, T: Two-phase nanofluid, R: Radiation).

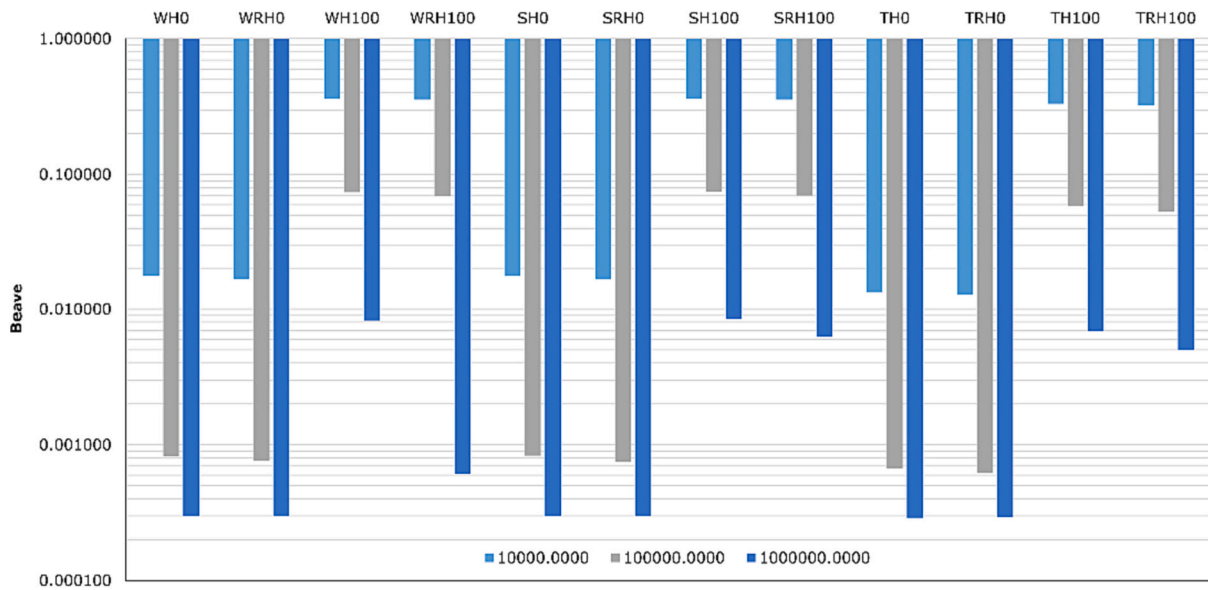


Fig. 5. The average Bejan number with respect to Rayleigh number with/without Ha for water, single-phase and two-phase conditions (W: water, H: Hartmann, S: single-phase nanofluid, T: Two-phase nanofluid, R: Radiation).

5.1. Heat transfer and second law of thermodynamics analyses

Fig. 3 illustrates the variation of average Nusselt number (Nu_{ave}) concerning the Rayleigh number (Ra) for different solving methods (single-phase and two-phase) applied to both water and nanofluid while considering the influence of a magnetic field and surface radiation in the calculations. The graph demonstrates that as Ra increases, the heat transfer rate also increases due to enhanced convection mechanisms. Modeling the nanofluid reveals its superior heat transfer capability when compared to the base fluid (water). Additionally, it is evident that thermal radiation plays a significant role in promoting heat transfer, leading to higher Nu_{ave} values. However, the considered vector of the magnetic field has a negative effect, moderating the fluid flow and consequently reducing the heat transfer rate. For instance, at $Ra = 10^5$, the Nu_{ave} decreases by approximately 1.7 % for water when Ha increases from 0 to 100. Moreover, for both single-phase and two-phase nanofluid models, the presence of the magnetic field leads to a decrease in Nu_{ave} by about 2.2 %. Also, it is worth noting that thermal radiation helps partially counteract the adverse effects of the strong magnetic field on heat transfer. At lower Ra values, the effect of surface radiation is more pronounced since the convection mechanism is comparatively weaker than the radiation mechanism. As Ra increases, the two-phase heat transfer modeling incurs a higher computational cost without significant differences. However, at higher Ra values, the two-phase nanofluid models exhibit improved performance in heat transfer modeling. At $Ra = 10^5$ and $Ra = 10^6$, the Nu_{ave} values for the two-phase nanofluid models are >5 % higher than those for water. Overall, the findings suggest that the nanofluid and the inclusion of thermal radiation can enhance heat transfer rates, while the presence of a magnetic field has a moderating effect on the fluid flow and heat transfer.

Increasing the Hartmann number acts like a braking force on the fluid flow and causes a decrease in the fluid velocity and heat transfer rate (see black square symbol and green triangle symbol). The radiation effect is positive on the heat transfer because as seen from Eq. (3), the radiation term (S_r in Eq. (3)) increases the values of right-hand side of energy equation. This leads to an increase in the heat transfer rate (In fact, the product of the fluid velocity in the temperature gradient increases). In this case, see green triangle and yellow triangle symbols. This act similar to increasing the Rayleigh number. The use of two-phase nanofluid models becomes more beneficial at higher Ra values, where it

leads to notable improvements in heat transfer modeling compared to single-phase models and water.

Fig. 4 depicts the logarithmic scale variation of entropy generation number with respect to Rayleigh number (Ra) for different conditions, including water, single-phase, and two-phase models, considering the presence or absence of a magnetic field (Ha). The graph shows that entropy generation increases with higher Ra values due to the increased particle movements within the system. Particularly, at $Ra = 10^6$, the system experiences a significant surge in entropy generation, acting as an actuator for enhancing entropy production. Moreover, both thermal radiation and the magnetic field contribute to the increased entropy generation in the system. At $Ra = 10^6$, thermal radiation alone leads to an 18 % increase in entropy generation, while the presence of the magnetic field, along with two-phase modeling, results in a substantial 78 % increase in entropy generation. Furthermore, the addition of nanoparticles to the fluid (nanofluid) further contributes to increased system irreversibility, leading to higher entropy generation. Overall, the results indicate that entropy generation is influenced by the Rayleigh number, thermal radiation, magnetic field, and the presence of nanoparticles. High Ra values, thermal radiation, and the magnetic field significantly promote entropy production in the system, underscoring the importance of considering these factors in the analysis of entropy generation in such complex fluid systems. According to the last term in Eq. (21), entropy generation is proportional to square power of Hartmann number. Therefore, entropy generation increases when Hartmann number increases from 0 (black square symbol) to 100 (green triangle symbol). Also, according to Eqs. (10) and (21), the ratio of nanofluid thermal conductivity to fluid thermal conductivity (k_{nf}/k_f) increases with increasing the particle volume fraction and then entropy generation increases when (k_{nf}/k_f) increases.

Fig. 5 presents logarithmic scale of the average Bejan number (Be) variation with respect to Rayleigh number (Ra) for different conditions, including water, single-phase, and two-phase models, considering the presence or absence of a magnetic field (Ha). The graph reveals that the Bejan number decreases as Ra increases, indicating that convection becomes the dominant mechanism at higher Rayleigh numbers. This suggests that as the flow becomes more convective, the Bejan number decreases, signifying the enhancement of heat transfer within the system. Additionally, thermal radiation aids in facilitating the movement of particles inside the medium. However, the magnetic field has a strong

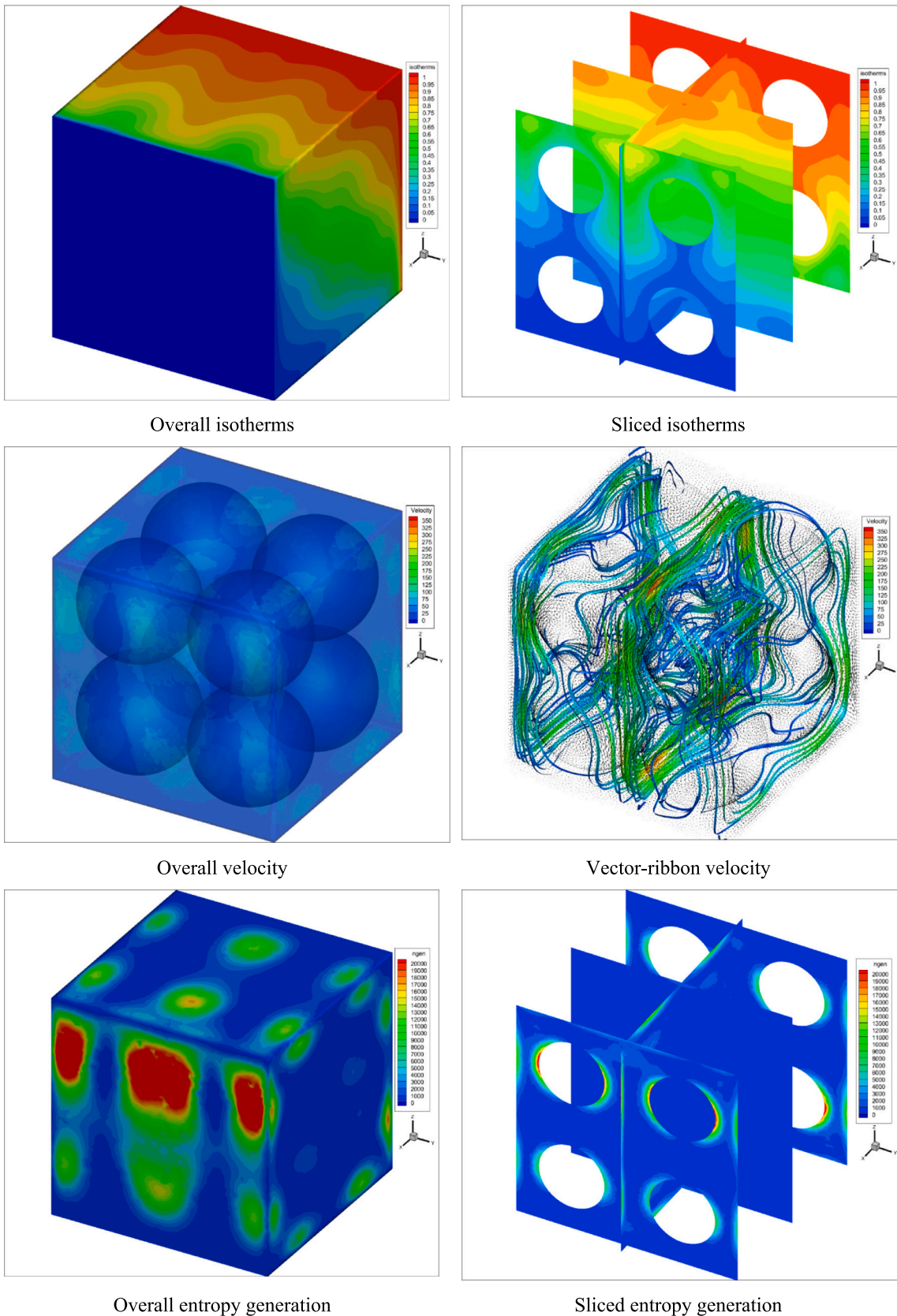


Fig. 6. Contour of isotherms, velocity, and entropy for nanofluid at $Ra = 10^6$.

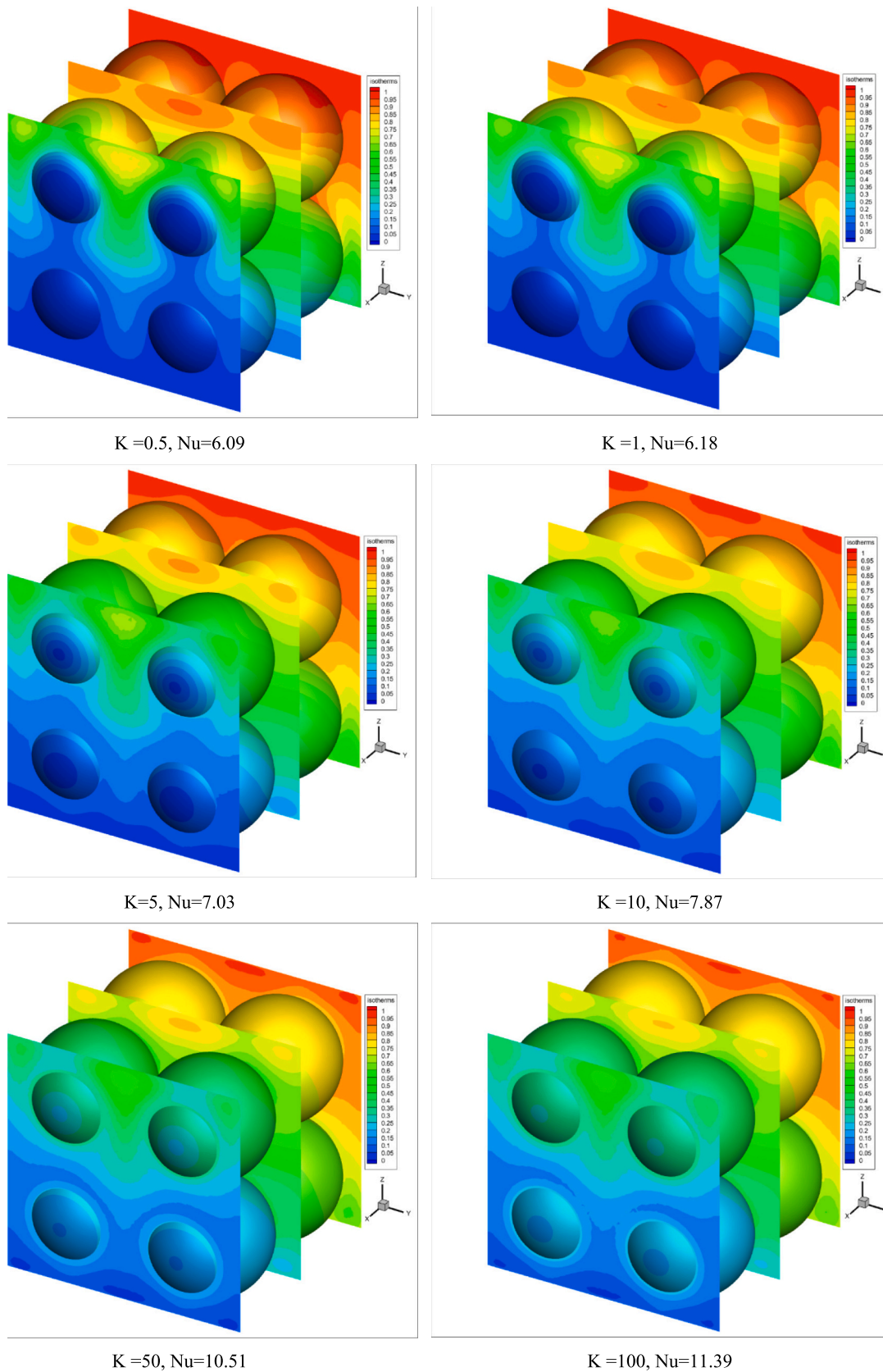


Fig. 7. The effect of thermal conductivity ratio ($K = 0.5, 1, 5, 10, 50, 100$) on average Nusselt number at $Ra = 10^6$ for two-phase nanofluid model.

effect on lower Rayleigh numbers. At lower Ra values, the application of a magnetic field leads to a significant increase in the Bejan number, even up to 100 %. This indicates that the convection mechanism is almost halted, and the fluid behaves more like a semiconductive solid under the influence of the magnetic field. Overall, the results demonstrate that convection is the dominant mechanism at higher Ra values, while the presence of a magnetic field has a profound effect on the Bejan number, especially at lower Rayleigh numbers. Thermal radiation, on the other hand, plays a more supportive role in enhancing the overall heat transfer within the system. As seen from this figure, at low Ra values (i.e., $Ra = 1e4$) the effect of Hartmann number is significant on the Bejan number. For example, the average Bejan number increases from approximately 0.02 to 0.36 while Hartmann number increases from 0 to 100 for single phase nanofluid without radiation effect. But, at high Ra values (i.e. $Ra = 1e6$), this effect is negligible (all values of average Bejan number are close to 0.01). The reason for this behavior is clear according to the last term of Eq. (21) and Eq. (23).

Fig. 6 presents the contours of isotherms, velocity (stream traces), and entropy generation for the nanofluid-filled enclosure at $Ra = 10^6$. The simulation is based on the two-phase model and includes the effects of thermal radiation while excluding the influence of the magnetic field. The isotherms contour reveals that the presence of pebbles enhances heat transfer, promoting the conducting heat transfer mechanism. Pebbles near the cold wall heat up, while those close to the hot wall cool down. The configuration of the pebbles, along with fluid circulation, results in fluid movement. The buoyancy force near the walls causes the fluid to rise parallel to the hot wall and fall near the cold wall. In the upper and lower sections of the cavity, density variations in the vertical direction led to stratified flow, as evident in the velocity contours. The contour of overall and sliced entropy generation indicates that entropy increases in the spaces near the contact regions between the pebbles. These contact regions introduce contractions and expansions in the fluid flow, increasing velocity and consequently the viscous model. The red regions in the overall entropy generation contour represent areas where the direction of the fluid changes. Specifically, these regions include the upper row of pebbles near the cold wall and the lower row of pebbles near the hot wall. Overall, Fig. 6 provides valuable insights into the distribution of temperature, velocity, and entropy generation in the nanofluid-filled enclosure at $Ra = 10^6$. The presence of pebbles, the flow patterns near the walls, and the contact regions between pebbles significantly influence heat transfer and entropy generation, making the study relevant for understanding and optimizing thermal performance in such complex systems.

Fig. 7 illustrates the effect of the solid-to-fluid thermal conductivity ratio (K) on the average Nusselt number (Nu_{ave}) at $Ra = 10^6$ for the two-phase nanofluid model. Different values of K are considered: $K = 0.5, 1, 5, 10, 50,$ and 100 . The reference calculation in the study is based on $K = 1$, representing the solid pebbles behaving as faithful solid regions, influencing fluid flow and heat transfer. From Fig. 7, it is evident that increasing the value of K leads to an increase in heat transfer. When K is >1 , the faces of the pebbles located near the walls enhance the heat transfer from the wall, resulting in an improved convection mechanism. On the other hand, for K values <1 , the heat transfer by the pebbles decreases, as their effect on the convection mechanism becomes minor. In summary, the thermal conductivity ratio (K) has a significant impact on heat transfer within the system. Higher K values promote better heat transfer, especially when $K > 1$, where the faces of the pebbles near the walls play a crucial role in enhancing the convection mechanism. Conversely, for $K < 1$, the heat transfer by the pebbles diminishes, as their influence on the convection mechanism becomes less significant. These findings emphasize the importance of considering the solid-to-fluid thermal conductivity ratio in the analysis of heat transfer and fluid flow in complex systems involving pebble beds and nanofluids.

6. Conclusion

This study utilized a finite volume method to investigate heat transfer, natural convection, and entropy generation in a 3D cubic enclosure filled with water and Al_2O_3 -water nanofluid containing structured conductive pebbles as a packed bed chamber. The system was heated and cooled from the sides, and natural convection was induced in the presence of a magnetic field and surface radiation. The governing equations for both single-phase and two-phase nanofluid models were solved using a non-dimensional method in ANSYS Fluent. The results were validated through quantitative and qualitative comparisons with prior numerical data, confirming the accuracy and reliability of the finite volume method for analyzing such complex problems involving nanofluids. The two-phase flow models yielded meaningful results for nanofluid modeling purposes. Key findings from the parametric analysis include:

- Both the Nu_{ave} and N_{gen} experience an increase with higher Rayleigh number (Ra), signifying that elevated Ra values amplify heat transfer across all sections of the system (as depicted in Figs. 3 and 4).
- The presence of a magnetic field (Hartmann number) decreases convective heat transfer, suggesting that the magnetic field can be used as a flow moderator to control heat transfer rates.
- The average Bejan number (Be) increases with Hartmann number and decreases with Rayleigh number (Fig. 5). At low Ra values, conduction dominates as the main heat transfer mode.
- The inclusion of pebbles enhances heat transfer due to the conducting heat transfer mechanism. Increasing the solid material thermal conductivity further augments heat transfer, as the high surface area-to-volume ratio of the spherical pebbles ensures effective heat exchange and minimizes thermal losses (Figs. 6, 7).
- The substantial alignment between our results and prior numerical data, both quantitatively and qualitatively, instills confidence in the efficacy of the Finite Volume Method (FVM) integrated within ANSYS Fluent to tackle intricate problems. This includes scenarios where two-phase flow models yield significant outcomes, particularly for the modeling of nanofluids.

For future research, investigating the impact of pebble size on the system's thermal performance could be beneficial. The modularity of the pebble bed design allows for easy expansion or contraction of the storage capacity, making it suitable for various applications, from small-scale residential systems to large-scale grid-level storage installations. Understanding the influence of pebble size on thermal behavior could optimize the design for different energy storage requirements.

CRedit authorship contribution statement

Mehdi Hashemi-Tilehnoee: Conceptualization, Methodology, Software, Writing, Original draft preparation.

Seyyed Masoud Seyyedi: Validating, Original draft preparation, Reviewing and Editing.

Elena Palomo Del Barrio: Conceptualization, Reviewing and Editing, Supervising.

Mohsen Sharifpur: Conceptualization, Reviewing and Editing.

Declaration of Generative AI and AI-assisted technologies in the writing process

Statement: During the preparation of this work the author(s) used ChatGPT in order to editing and improving the text. After using this tool/service, the author(s) reviewed and edited the content as needed and take(s) full responsibility for the content of the publication.

Declaration of competing interest

The authors declare that they have no known competing financial interests or personal relationships that could have appeared to influence the work reported in this paper.

Data availability

No data was used for the research described in the article.

References

- Y. Qu, L. Wang, X. Lin, H. Ling, Y. Bai, S. Zhang, H. Chen, Heat transfer characteristics of mixed convection in packed beds, *Chem. Eng. Sci.* 255 (2022), 117679, <https://doi.org/10.1016/j.ces.2022.117679>.
- M.J. Li, B. Jin, J.J. Yan, Z. Ma, M.J. Li, Numerical and experimental study on the performance of a new two-layered high-temperature packed-bed thermal energy storage system with changed-diameter macro-encapsulation capsule, *Appl. Therm. Eng.* 142 (2018) 830–845, <https://doi.org/10.1016/j.applthermaleng.2018.07.026>.
- J. Chen, X. Li, X. Huai, Experimental study on the heat transfer of gas with coagulative particles flowing through a packed granular bed filter, *Appl. Therm. Eng.* 141 (2018) 906–912, <https://doi.org/10.1016/j.applthermaleng.2018.06.050>.
- S. Bu, J. Wang, W. Sun, Z. Ma, L. Zhang, L. Pan, Numerical and experimental study of stagnant effective thermal conductivity of a graphite pebble bed with high solid to fluid thermal conductivity ratios, *Appl. Therm. Eng.* 164 (2020), 114511, <https://doi.org/10.1016/j.applthermaleng.2019.114511>.
- H.P.A. Calis, J. Nijenhuis, B.C. Paikert, F.M. Dautzenberg, C.M. Van Den Bleek, CFD modeling and experimental validation of pressure drop and flow profile in a novel structured catalytic reactor packing, *Chem. Eng. Sci.* 56 (2001) 1713–1720, [https://doi.org/10.1016/S0009-2509\(00\)00400-0](https://doi.org/10.1016/S0009-2509(00)00400-0).
- J. Yang, J. Wang, S. Bu, M. Zeng, Q. Wang, A. Nakayama, Experimental analysis of forced convective heat transfer in novel structured packed beds of particles, *Chem. Eng. Sci.* 71 (2012) 126–137, <https://doi.org/10.1016/j.ces.2011.12.005>.
- S. Bu, Z. Li, Z. Ma, W. Sun, L. Zhang, D. Chen, Numerical study of natural convection effects on effective thermal conductivity in a pebble bed, *Ann. Nucl. Energy* 144 (2020), 107524, <https://doi.org/10.1016/j.anucene.2020.107524>.
- O. Laguerre, S. Ben Amara, G. Alvarez, D. Flick, Transient heat transfer by free convection in a packed bed of spheres: comparison between two modelling approaches and experimental results, *Appl. Therm. Eng.* 28 (2008) 14–24, <https://doi.org/10.1016/j.applthermaleng.2007.03.014>.
- Y. Qu, L. Wang, X. Lin, H. Chen, S. Zhang, H. Ling, Y. Bai, Mixed convective heat transfer characteristics and mechanisms in structured packed beds, *Particuology* 82 (2023) 122–133, <https://doi.org/10.1016/j.partic.2023.01.014>.
- A. Abidi, L. Kolsi, M.N. Borjini, H. Ben Aissia, Effect of radiative heat transfer on three-dimensional double diffusive natural convection, *Numer. Heat Transf. Part A Appl.* 60 (2011) 785–809, <https://doi.org/10.1080/10407782.2011.627797>.
- H. Sun, E. Chénier, G. Lauriat, Effect of surface radiation on the breakdown of steady natural convection flows in a square, air-filled cavity containing a centered inner body, *Appl. Therm. Eng.* 31 (2011) 1252–1262, <https://doi.org/10.1016/j.applthermaleng.2010.12.028>.
- L. Kolsi, A. Abidi, C. Maatki, M.N. Borjini, H. Ben Aissia, Combined radiation-natural convection in three-dimensional vertical cavities, *Therm. Sci.* 15 (2011) 383–390, <https://doi.org/10.2298/TSCI101209081K>.
- G. Yang, J.Y. Wu, Effects of natural convection, wall thermal conduction, and thermal radiation on heat transfer uniformity at a heated plate located at the bottom of a three-dimensional rectangular enclosure, *Numer. Heat Transf. Part A Appl.* 69 (2016) 589–606, <https://doi.org/10.1080/10407782.2015.1090238>.
- M. Parmananda, A. Dalal, G. Natarajan, Unified framework for buoyancy induced radiative-convective flow and heat transfer on hybrid unstructured meshes, *Int. J. Heat Mass Transf.* 126 (2018) 908–925, <https://doi.org/10.1016/j.ijheatmasstransfer.2018.05.092>.
- A. Nee, Hybrid lattice Boltzmann—finite difference formulation for combined heat transfer problems by 3D natural convection and surface thermal radiation, *Int. J. Mech. Sci.* 173 (2020), <https://doi.org/10.1016/j.ijmecsci.2020.105447>.
- S.M. Seyyedi, M. Hashemi-Tilehnoee, E. Palomo del Barrio, A.S. Dagonchi, S. M. Ghadami, M. Sharifpur, Electro-enhanced natural convection analysis for an Al2O3-water-filled enclosure by considering the effect of thermal radiation, *Numer. Heat Transf. Part A Appl.* (2023) 1–20, <https://doi.org/10.1080/10407782.2023.2243380>.
- J. Macak, C. Goniva, S. Radl, Predictions of the P1 approximation for radiative heat transfer in heterogeneous granular media, *Particuology* 82 (2023), <https://doi.org/10.1016/j.partic.2023.01.003>.
- G. Wang, Z. Zhang, R. Wang, Z. Zhu, A review on heat transfer of nanofluids by applied electric field or magnetic field, *Nanomaterials* 10 (2020), <https://doi.org/10.3390/nano10122386>.
- M. Battira, R. Bessaïh, Three-dimensional natural convection in the horizontal Bridgman configuration under various wall electrical conductivity and magnetic field, *Numer. Heat Transf. Part A Appl.* 55 (2009), <https://doi.org/10.1080/10407780802603113>.
- A. Purusothaman, H.F. Öztop, N. Nithyadevi, N.H. Abu-Hamdeh, 3D natural convection in a cubical cavity with a thermally active heater under the presence of an external magnetic field, *Comput. Fluids* 128 (2016), <https://doi.org/10.1016/j.compfluid.2016.01.011>.
- C. Maatki, K. Ghachem, L. Kolsi, A.K. Hussein, M.N. Borjini, H. Ben Aissia, Inclination effects of magnetic field direction in 3D double-diffusive natural convection, *Appl. Math. Comput.* 273 (2016), <https://doi.org/10.1016/j.amc.2015.09.043>.
- F. Selimefendil, H.F. Öztop, Role of magnetic field and surface corrugation on natural convection in a nanofluid filled 3D trapezoidal cavity, *Int. Commun. Heat Mass Transf.* 95 (2018), <https://doi.org/10.1016/j.icheatmasstransfer.2018.05.006>.
- M. Sheikholeslami, S.A. Shehzad, Z. Li, Water based nanofluid free convection heat transfer in a three dimensional porous cavity with hot sphere obstacle in existence of Lorenz forces, *Int. J. Heat Mass Transf.* 125 (2018), <https://doi.org/10.1016/j.ijheatmasstransfer.2018.04.076>.
- H. Sajjadi, A.A. Delouei, M. Atashafrooz, M. Sheikholeslami, Double MRT lattice Boltzmann simulation of 3-D MHD natural convection in a cubic cavity with sinusoidal temperature distribution utilizing nanofluid, *Int. J. Heat Mass Transf.* 126 (2018), <https://doi.org/10.1016/j.ijheatmasstransfer.2018.05.064>.
- A.A.A.A. Al-Rashed, K. Kalidasan, L. Kolsi, A. Aydi, E.H. Malekshah, A.K. Hussein, P. Rajesh Kanna, Three-dimensional investigation of the effects of external magnetic field inclination on laminar natural convection heat transfer in CNT-water nanofluid filled cavity, *J. Mol. Liq.* 252 (2018), <https://doi.org/10.1016/j.molliq.2018.01.006>.
- L. Kolsi, H.F. Öztop, K. Ghachem, M.A. Almeshaal, H.A. Mohammed, H. Babazadeh, N. Abu-Hamdeh, Numerical study of periodic magnetic field effect on 3D natural convection of MWCNT-water/nanofluid with consideration of aggregation, *Processes* 7 (2019), <https://doi.org/10.3390/PR7120957>.
- Z. Boulahia, C. Boulahia, R. Sehaqui, Three-dimensional (3D) visualization and two-dimensional (2D) second law analysis of magnetohydrodynamic (MHD) free convection inside cubical enclosure packed with hybrid nanofluid containing a circular heating cylinder: effect of inclined magnetic field, *Arab. J. Sci. Eng.* 46 (2021), <https://doi.org/10.1007/s13369-020-05293-w>.
- S.E. Ahmed, H.M. Elshehaby, H.F. Öztop, Natural convection of three-dimensional non-Newtonian nanofluids with Marangoni effects and inclined magnetic fields, *Int. Commun. Heat Mass Transf.* 137 (2022), <https://doi.org/10.1016/j.icheatmasstransfer.2022.106288>.
- M. Sheikholeslami, M. Seyednezhad, Simulation of nanofluid flow and natural convection in a porous media under the influence of electric field using CVFEM, *Int. J. Heat Mass Transf.* 120 (2018), <https://doi.org/10.1016/j.ijheatmasstransfer.2017.12.087>.
- ANSYS FLUENT 13 User's Guide, *Ansys Fluent Theory Guide*, 2013.
- A. El Jerry, N. Hidouri, M. Magherbi, A. Ben Brahim, Effect of an external oriented magnetic field on entropy generation in natural convection, *Entropy* 12 (2010), <https://doi.org/10.3390/entropy12061391>.
- M. Hashemi-Tilehnoee, A.S. Dagonchi, S.M. Seyyedi, M. Sharifpur, Magneto-fluid dynamic and second law analysis in a hot porous cavity filled by nanofluid and nano-encapsulated phase change material suspension with different layout of cooling channels, *J. Energy Storage* 31 (2020), <https://doi.org/10.1016/j.est.2020.101720>.
- M. Hashemi-Tilehnoee, E. Palomo del Barrio, Magneto laminar mixed convection and entropy generation analyses of an impinging slot jet of Al2O3-water and Novoc-649, *Therm. Sci. Eng. Prog.* 36 (2022), <https://doi.org/10.1016/j.tsep.2022.101524>.
- A.M. Ali, M. Angelino, A. Rona, Physically consistent implementation of the mixture model for modelling nanofluid conjugate heat transfer in minichannel heat sinks, *Appl. Sci.* 12 (2022), <https://doi.org/10.3390/app12147011>.
- M. Hashemi-Tilehnoee, E.P. del Barrio, S.M. Seyyedi, Magneto-turbulent natural convection and entropy generation analyses in liquid sodium-filled cavity partially heated and cooled from sidewalls with circular blocks, *Int. Commun. Heat Mass Transf.* 134 (2022), 106053, <https://doi.org/10.1016/j.icheatmasstransfer.2022.106053>.
- M. Hashemi-Tilehnoee, S.M. Seyyedi, E. Palomo del Barrio, M. Sharifpur, Heat transfer intensification of NEPCM-water suspension filled heat sink cavity with notches cooling tubes by applying the electric field, *J. Energy Storage* 59 (2023), <https://doi.org/10.1016/j.est.2022.106492>.
- S.M. Seyyedi, M. Hashemi-Tilehnoee, E. Palomo del Barrio, A.S. Dagonchi, M. Sharifpur, Analysis of magneto-natural-convection flow in a semi-annulus enclosure filled with a micropolar-nanofluid; a computational framework using CVFEM and FVM, *J. Magn. Magn. Mater.* 568 (2023), <https://doi.org/10.1016/j.jmmm.2023.170407>.
- A.A. Merrikh, J.L. Lage, Natural convection in an enclosure with disconnected and conducting solid blocks, *Int. J. Heat Mass Transf.* 48 (2005), <https://doi.org/10.1016/j.ijheatmasstransfer.2004.09.043>.
- I. Dincer, M.A. Rosen, Exergy: Energy, Environment and Sustainable Development, 2020, <https://doi.org/10.1016/B978-0-12-824372-5.09986-3>.
- M. Hashemi-Tilehnoee, S. Tashakor, A.S. Dagonchi, S.M. Seyyedi, M. Khaleghi, Entropy generation in concentric annuli of 400 kV gas-insulated transmission line, *Therm. Sci. Eng. Prog.* 19 (2020), <https://doi.org/10.1016/j.tsep.2020.100614>.

- [41] S.M. Seyyedi, M. Hashemi-Tilehnoee, M. Sharifpur, Impact of fusion temperature on hydrothermal features of flow within an annulus loaded with nanoencapsulated phase change materials (NEPCMs) during natural convection process, *Math. Probl. Eng.* 2021 (2021), <https://doi.org/10.1155/2021/4276894>.
- [42] S.S. Bu, J. Yang, M. Zhou, S.Y. Li, Q.W. Wang, Z.X. Guo, On contact point modifications for forced convective heat transfer analysis in a structured packed bed of spheres, *Nucl. Eng. Des.* 270 (2014), <https://doi.org/10.1016/j.nucengdes.2014.01.001>.
- [43] M. Pirmohammadi, Numerical study of turbulent magnetohydrodynamic convection of molten sodium with variable properties in a square cavity, *Therm. Sci.* 23 (2019) 3443–3454.
- [44] M. Pirmohammadi, Numerical study of turbulent free convection of liquid metal with constant and variable properties in the presence of magnetic field, *J. Heat Mass Transf. Res.* 6 (2019) 133–141.
- [45] T. Fusegi, J.M. Hyun, K. Kuwahara, B. Farouk, A numerical study of three-dimensional natural convection in a differentially heated cubical enclosure, *Int. J. Heat Mass Transf.* 34 (1991), [https://doi.org/10.1016/0017-9310\(91\)90295-P](https://doi.org/10.1016/0017-9310(91)90295-P).